Applied Catalysis A, General 704 (2025) 120378

Contents lists available at ScienceDirect

Applied Catalysis A, General

journal homepage: www.elsevier.com/locate/apcata

Oxidation of n-alkanes using TS-1 and H_2O_2: Effects of chain length and solvents

Seyeon Park [a], Maura Gibbs [b], Zhuoming Feng [a], Karen I. Goldberg [b], Daeyeon Lee [a], Raymond J. Gorte [a], John M. Vohs [a,*]

[a] Department of Chemical and Biomolecular Engineering, University of Pennsylvania, Philadelphia, PA 19104, USA
[b] Department of Chemistry, University of Pennsylvania, Philadelphia, PA 19104, USA

ARTICLE INFO

Keywords:
Alkane oxidation
Titanium silicate
TS-1
Zeolite
Plastic upcycling
Plastic recycling

ABSTRACT

The selective oxidation of n-C_8H_{18}, n-$C_{12}H_{26}$, n-$C_{16}H_{34}$, n-$C_{20}H_{42}$, and n-$C_{36}H_{74}$ was studied with a goal of using these as models to provide insight into how to functionalize polyolefins. Reactions were carried out using a TS-1 catalyst and H_2O_2 in a batch reactor with different cosolvents, including methanol, acetone, acetonitrile, methyl ethyl ketone, and methyl butyl ketone. Rates decreased with increasing alkane size, possibly due to the reduced solubility of larger alkanes into the water-rich phases. Cosolvents that promote the partitioning of alkanes in the aqueous phase increased the rates. ^{1}H NMR spectroscopy demonstrated that ketones were the primary products, although some alcohols also formed. There was preferential reaction at the 2 position in the alkanes, but reaction at central carbons was also observed. The results of this study suggest strategies for using this catalytic chemistry to functionalize polyolefins.

1. Introduction

Polyolefins, integral to countless products in modern society, pose a significant environmental challenge due to the immense difficulty associated with their disposal. Discarded polyolefins are usually either incinerated or placed in landfills, environmentally harmful practices that waste the valuable chemical energy stored within these polymers. This situation has sparked an intense research effort to find ways to recycle polyolefins into useful products. Most of these efforts involve cleaving C-C bonds to produce hydrocarbons with lower molecular weights that could be used as fuels or lubricants [1–6]. An important barrier to adopting this approach is the relatively low value of the resulting products, which may not offset the cost of processing and the hydrogen consumed in the reactions.

An alternative approach to chemically recycling these waste plastics involves converting the discarded polyolefins into new feedstocks for producing specialty polymers. For example, some polyolefin copolymers that contain functional groups have significantly greater value than conventional polyolefins because of their high toughness and adhesive properties [7]. By functionalizing waste polyolefins without decreasing their molecular weights, it is possible to repurpose the discarded materials for a wide range of applications. Mild oxidation to incorporate alcohol and ketone groups dramatically enhances the functionality [8]. The oxygen functionalities could also be modified with other functional groups to derive useful properties [9]. However, due to the chemical and thermal stability of polyolefins, partial oxidation, without additional C-C bond cleavage, is very difficult.

Recent publications have reported selective oxidation of C–H bonds in polyethylene, without chain scission or cross linking, using Ni- and Ru-based complexes as catalysts. For example, successful incorporation of hydroxyl, carbonyl, and alkyl chloride groups into polyethylene has been achieved using [Ni(Me_4Phen)$_3$](BPh_4)$_2$[10]. Hydroxylation occurs primarily at secondary C–H bonds and does not substantially change the molecular weight of the polymer. A subsequent study using a Ru complex circumvented chlorine incorporation and significantly enhanced the level of functionalization [7]. These results demonstrate that modification of polyolefins is possible. Applying these methods to waste polymers on the commercial scale, however, poses several challenges. The transition-metal complexes are expensive and difficult to separate from the products [11]. The catalysts are also sensitive to the reaction environment [12] and could be poisoned by the presence of impurities in the waste stream. There would be significant advantages to using an inexpensive, heterogeneous catalyst for this application.

The mild oxidation of small alkanes, without C-C bond cleavage,

* Corresponding author.
E-mail address: vohs@seas.upenn.edu (J.M. Vohs).

https://doi.org/10.1016/j.apcata.2025.120378
Received 3 March 2025; Received in revised form 23 May 2025; Accepted 26 May 2025
Available online 27 May 2025

using H_2O_2 and the titanium silicate catalyst, TS-1, offers a promising model for achieving partial oxidation of polyolefins [13,14]. TS-1 is a siliceous molecular sieve with the MFI structure that has some of the framework Si atoms replaced by Ti [15]. TS-1 is commercially used for the epoxidation of propylene [16]. For oxidation of small alkanes, reactions proceed under relatively mild conditions, typically between room temperature and ~350 K [13,14]. The presence of cosolvents, alongside the water accompanying H_2O_2, has been shown to increase the reaction rate[17], presumably by enhancing the solubility of the alkane in the aqueous phase where the H_2O_2 oxidant and TS-1 catalyst are located. Mechanistic studies have shown that the isolated Ti sites readily react with H_2O_2 to form Ti-peroxo complexes, which then react with alkane molecules within the zeolite pores to produce oxidized products [14,18].

Despite these promising results, there are important issues that need to be considered to enable mild oxidation of polymers using TS-1. First, there are questions about how a reaction of hydrophobic polymers can occur with an aqueous reactant, like H_2O_2. Second, TS-1 is a molecular sieve with sub-nanometer pores that may prevent polymers from accessing the active sites. Finally, we are not aware of studies in which TS-1 has been applied to oxidation of alkanes larger than n-$C_{13}H_{28}$[19].

In the present study, we set out to investigate the factors that influence the mild oxidation of large alkanes from n-C_8H_{18} (octane) to n-$C_{36}H_{74}$ (hexatriacontane) over TS-1. We compare reaction rates for different alkanes and examine the effect of different cosolvents. We show that alcohol and ketone functionalities are incorporated primarily at secondary carbons. Although rates decreased systematically with increasing molecular weight of the alkanes, our results suggest pathways for achieving mild oxidation of polyolefins.

2. Experimental section

2.1. Materials

The dodecane (n-$C_{12}H_{26}$), eicosane (n-$C_{20}H_{42}$), hydrogen-peroxide solution (50 wt% H_2O_2 in water), and 2-butanone (methyl ethyl ketone, MEK) used in this study were purchased from Sigma-Aldrich. Acetonitrile (CH_3CN), 2-hexanone ($CH_3COC_4H_9$, methyl butyl ketone, MBK), methanol (CH_3COH), acetone (CH_3COCH_3), and 2-propanol came from Fisher Chemical; octane (n-C_8H_{18}) and hexatriacontane (n-$C_{36}H_{74}$) were purchased from Thermo Scientific. Tetrapropyl ammonium hydroxide solution (TPAOH, 20–25 wt% in water) was purchased from TCI Chemicals. Hexadecane (n-$C_{16}H_{34}$) and acetonitrile-d_3 (CD_3CN) were obtained from Acros Organics. Deuterated $CDCl_3$ was purchased from Cambridge Isotope Laboratories. All chemicals were used as received.

The titanosilicate (TS-1(190)) used in some studies was purchased from ACS Materials. The vendor reports a Si/Ti ratio of 82. Characterization of the catalyst is summarized in Table S1 and Fig. S1. Briefly, X-ray diffraction (XRD) patterns depicted in Fig. S1a confirmed that the sample had the MFI structure. Scanning electron microscopy (SEM) images indicated that the crystallites were roughly spherical, with diameters of ~190 nm (Figures S1b and c). The pore volume of the sample, determined from the amount of n-hexane adsorbed at 10 torr and room temperature, was 0.16 cm^3/g, assuming a liquid density for n-hexane [20]. This volume is similar to what has been reported elsewhere for MFI zeolites and compares favorably to the theoretical value of 0.19 cm^3/g [21]. Diffuse Reflectance Infrared Fourier Transform (DRIFT) spectra of adsorbed CD_3CN, shown in Fig. S2, exhibited a clearly defined $\nu(C{\equiv}N)$ peak at 2295 cm^{-1}, indicative of framework Ti[22,23].

A second titanosilicate catalyst, TS-1(420), was also prepared for studying possible diffusion limitations. It was synthesized using a protocol reported in the literature and consisted of crystallites that were larger than that of the TS-1(190) sample[24]. The synthesis began by mixing 7.8 g of TPAOH with 13 g of deionized (DI) water, after which 9 g of TEOS was added dropwise with vigorous stirring until the mixture became clear. Separately, 300 μL of $Ti(OBu)_4$ was dissolved in 5 mL of 2-propanol, followed by 2 h of stirring. The Ti-containing solution was then added dropwise to the TEOS-containing solution, followed by vigorous stirring to achieve a clear solution. After transferring the mixture to a Teflon-lined, stainless-steel autoclave, the batch was heated to 453 K for 40 h. Upon cooling, the product was repeatedly washed in DI water and dried at 348 K in air overnight. The resultant powder was calcined at 823 K for 5 h in flowing air to remove the TPAOH template. The nominal Si/Ti ratio for the synthesis was 54. As shown in Fig. S3 and Table S1, the particle size and the pore volume were 420 nm and 0.16 cm^3/g, respectively.

2.2. Reactivity tests

Most alkane-oxidation reactions were performed in a flat-bottom, round flask equipped with a reflux condenser to minimize solvent evaporation. Between 0.01 and 1 g of catalyst were loaded into the reactor with 10 mL of a cosolvent, 10 mL of H_2O_2 solution, and between 1 and 5 g of alkane reactant. Under these conditions, there were always two liquid phases, an organic-rich phase and an aqueous phase, with H_2O_2 in large excess. The TS-1 catalysts remained in the aqueous phase. The reactions were performed under vigorous stirring. Small aliquots of the reaction mixture were periodically extracted, and the organic layers were collected over the course of the reaction to determine the hydrocarbon products and conversions.

Some reactions were also performed in a sealed, stainless-steel, batch reactor. Although it was not possible to monitor alkane conversion as a function of time in this reactor, conversions for a given contact time were found to be essentially the same as that measured in the flat-bottomed flask. Because the reactor was sealed, the pressure increased with time due to decomposition of H_2O_2 into O_2 and H_2O, which in turn allowed us to measure the efficiency of H_2O_2 utilization.

The rate measurements and initial analysis of the products were accomplished by gas chromatography-mass spectrometry (GC-MS, QP-5000, Shimadzu, using an HP-Innowax capillary column, Agilent Technologies). The organic component of the product aliquots was mixed with toluene and analyzed to determine the hydrocarbon conversion. Rates were calculated by dividing the amounts of alkane that reacted by the reaction time and the mass of catalyst. For these measurements, the alkane conversions varied from 0.1 % to 15 %. Blank tests conducted at 348 K without catalyst exhibited no reaction.

In some cases, products were also analyzed using ^1H nuclear magnetic resonance (NMR) spectroscopy to determine the type and position of the functional groups. 2D ^1H–^{13}C NMR spectra using Heteronuclear Single Quantum Coherence (HSQC) and Heteronuclear Multiple Bond Correlation (HMBC) experiments were also conducted. The spectra were acquired on a Bruker NEO 600 MHz spectrometer, equipped with a Prodigy probe, using residual solvent peaks as references (^1H NMR: $CDCl_3$ at 7.26 ppm; ^{13}C NMR: $CDCl_3$ at 77.16 ppm). All NMR spectra were recorded at ambient temperature, with chemical shifts (δ) reported in ppm. For these measurements, between 10 and 15 mg of the organic layer in the reaction mixture was dissolved in $CDCl_3$. For eicosane and hexatriacontane reactions, the organic layers were first dried by evacuation for 2 h, after which the solids were sonicated in $CDCl_3$. The aqueous layers of the reactant mixture showed no significant ^1H NMR signal that could be associated with hydrocarbons. The obtained spectra were analyzed with reference to the spectral database for organic compounds organized by National Institute of Advanced Industrial Science and Technology, Japan.

3. Results

3.1. Reaction rates

The initial reaction measurements were performed with n-$C_{16}H_{34}$ at 348 K in the flat-bottom-flask reactor using acetonitrile and MEK as the cosolvents and TS-1(190) as the catalyst. As shown in Fig. 1, the

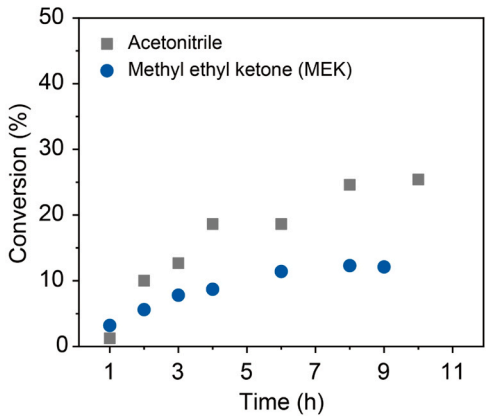

Fig. 1. Conversion of n-$C_{16}H_{34}$ oxidation as a function of reaction time using acetonitrile and methyl ethyl ketone cosolvent. (Reaction conditions: 3 g n-$C_{16}H_{34}$, 1 g TS-1, 10 mL H_2O_2 solution, and 10 mL acetonitrile; 5 g n-$C_{16}H_{34}$, 0.05 g TS-1, 10 mL H_2O_2 solution, and 10 mL MEK).

conversions increased with time but leveled off to a constant value after approximately 6–8 h. The decreased hydrocarbon reaction rate was due to consumption of H_2O_2 and not to catalyst deactivation. First, the catalyst could be reused, without loss of activity, by simply washing in a solvent. Second, replicating the reaction in the stainless-steel reactor showed that the pressure increased with time due to H_2O_2 decomposition. As shown in Figures S4 and S5, the reactor pressure increased steadily with time for reaction in either cosolvent. Assuming that the pressure rise reflects only decomposition of H_2O_2 into H_2O and O_2, the plateau in pressure marks the complete depletion of the oxidant. The fraction decomposed at any given time can be calculated simply by dividing the pressure at that time by the plateau pressure. In this manner, only about 30 % of the initial H_2O_2 remained after 8 h reaction in either cosolvent, suggesting that the conversions in Fig. 1 leveled off due to depletion of the H_2O_2.

We also examined the effect of catalyst loading and the amount of hydrocarbon charged to the reactor. The conversions after short reaction times were found to increase linearly with the amounts of TS-1(190) catalyst and inversely with the amounts of hydrocarbon. Specifically, in acetonitrile, decreasing the initial amount of hexadecane from 3.0 g to 1.5 g doubled the conversion. Similarly, for 1.5 g of hexadecane, increasing the catalyst loading from 1 g to 2 g resulted in a 2-fold increase in conversion. No conversion was observed in the absence of a catalyst. Under the conditions used here, the reaction mixture consisted of two liquid phases, an organic solvent-rich liquid and a water-rich liquid. Because reaction occurs on the TS-1, which segregates to the aqueous-rich phase[18], rates are proportional to the amount of catalyst. Because the concentration of n-$C_{16}H_{34}$ in the aqueous phase will be determined by the phase equilibrium, independent of how much n-$C_{16}H_{34}$ was initially added to the reactor, the hydrocarbon concentration at the catalyst will be essentially constant for lower conversions.

These results imply that specific, intrinsic reaction rates can be calculated from the conversions at short times for which the H_2O_2 concentration remains high in the aqueous phase. For n-$C_{16}H_{34}$ at 348 K in acetonitrile, the specific rate was found to be $(7.0 \pm 1.5)\times 10^{16}$ molecules g^{-1} s^{-1}. At conversions greater than 5 %, the product analysis showed some products had undergone a second oxidation; but the extent to which difunctional products were formed was minor. Even at 10 % conversion, the amount of difunctional products was only about 1 %. The selectivity to difunctional products increased with conversion, as expected for a series reaction. Product analysis by GC-MS also did not provide any evidence for C-C bond scission reactions occurring for the conditions used in this study.

To determine the effect of hydrocarbon size, oxidation measurements were performed with other linear alkanes, ranging from n-C_8H_{18} to n-$C_{36}H_{74}$. The reactions were again performed with acetonitrile as the cosolvent at 348 K; the initial amounts of TS-1(190) catalyst and hydrocarbon added to the reactor, as well as the reaction time, were varied to maintain the conversions to less than 10 %. The results are shown in Table 1, with the specific rates plotted as a function of the hydrocarbon length in Fig. 2. The specific rates decreased in an exponential manner with increasing hydrocarbon size, from $(5.7 \pm 0.7)\times 10^{17}$ molecules g^{-1} s^{-1} for n-C_8H_{18} to $(4.1 \pm 1.2)\times 10^{14}$ molecules g^{-1} s^{-1} for n-$C_{36}H_{74}$.

The likely reason for why rates decreased with alkane chain length is either the limited solubilities of the alkanes in the aqueous phase or diffusion limitations due to molecular size of the reactant. To examine the role of solubility, we examined reaction rates in the presence of different cosolvents. MEK was of particular interest since previous work demonstrated enhanced oxidation rates for small hydrocarbons in TS-1 when using MEK compared to acetonitrile[25]. Rate measurements were again performed for each of the hydrocarbons in MEK at 348 K, using TS-1(190) as the catalyst, with results reported in Table 2 and plotted in Fig. 3. As in the case when acetonitrile was the cosolvent, rates again decreased with increasing hydrocarbon chain length in a nearly exponential manner; however, the rates were, on average, about 50 times higher in MEK.

We investigated cosolvent effects further by measuring oxidation rates for n-$C_{12}H_{26}$ over TS-1(190) at 348 K, using methanol, acetone, and MBK as the cosolvents. These reactions were conducted in the stainless-steel batch reactor to contain the volatile solvents. Reaction rates for each of the five cosolvents tested are reported in Table 3. No reaction of the n-$C_{12}H_{26}$ was observed with either methanol or acetone under these reaction conditions. Although some oxidation of the butyl group was observed with MBK, making it unsuitable as a cosolvent for this application, oxidation of the butyl group proceeded more slowly than that of n-$C_{12}H_{26}$, allowing for measurement of reaction rates for n-$C_{12}H_{26}$. Oxidation rates in MBK were found to be more than 30 % higher than those in MEK.

We propose that the variations in rate for the organic solvents are due to them acting as cosolvents that enhance the solubility of the alkane reactant in the water phase which contains the H_2O_2 oxidant and the TS-1 catalyst. While it would be useful to know how effective each cosolvent is at increasing the alkane solubility in the water phase, this information is not available in the literature. What is available, however, are coefficients for partitioning of the organic solvents into the two phases of the octanol-water system[26]. These partition coefficient (P) values are listed in Table 3. We propose that these P values can be used as a surrogate for correlating how the cosolvent increases the alkane solubility in water. The data in Table 3 do indeed demonstrate a correlation and show that polar cosolvents that are more soluble in octanol are the most effective at enhancing the n-$C_{12}H_{26}$ reaction rate. This may be due to the fact that these cosolvents contain both nonpolar ethyl or butyl groups that can interact with the alkane, and polar carbonyl groups that still afford them solubility in the aqueous phase. The rates for n-$C_{12}H_{26}$ oxidation are also plotted as a function of *P* in Fig. 4 and indicate that there is a strong correlation between the reaction rate and the partition coefficient. Higher rates were observed in those cosolvents that had a higher affinity for the organic phase. The relationship

Table 1
Oxidation rate for octane (n-C_8H_{18}), dodecane (n-$C_{12}H_{26}$), hexadecane (n-$C_{16}H_{34}$), eicosane (n-$C_{20}H_{42}$) and hexatriacontane (n-$C_{36}H_{74}$) using acetonitrile cosolvent at 348 K.

Reactant	Reaction Rate (molecules g^{-1} s^{-1})
n-C_8H_{18}	$(5.7 \pm 0.7)\times 10^{17}$
n-$C_{12}H_{26}$	$(2.4 \pm 0.9)\times 10^{17}$
n-$C_{16}H_{34}$	$(7.0 \pm 1.5)\times 10^{16}$
n-$C_{20}H_{42}$	$(3.4 \pm 1.6)\times 10^{16}$
n-$C_{36}H_{74}$	$(4.1 \pm 1.2)\times 10^{14}$

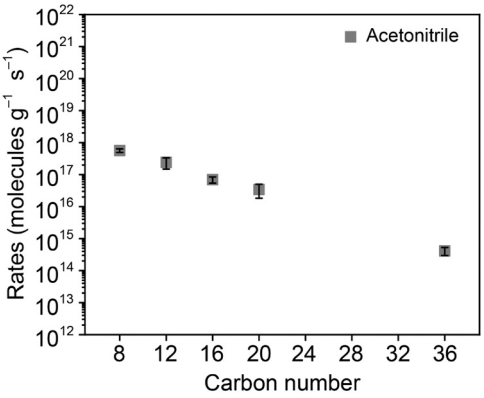

Fig. 2. Oxidation rates for linear alkanes ranging from octane (n-C_8H_{18}) to hexatriacontane (n-$C_{36}H_{74}$) in acetonitrile. (Error bars indicate standard deviation.).

Table 2
Oxidation rate for octane (n-C_8H_{18}), dodecane (n-$C_{12}H_{26}$), hexadecane (n-$C_{16}H_{34}$), eicosane (n-$C_{20}H_{42}$) and hexatriacontane (n-$C_{36}H_{74}$) using MEK cosolvent at 348 K.

Reactant	Reaction Rate (molecules g^{-1} s^{-1})
n-C_8H_{18}	$(3.6 \pm 0.3) \times 10^{19}$
n-$C_{12}H_{26}$	$(2.1 \pm 0.1) \times 10^{19}$
n-$C_{16}H_{34}$	$(2.1 \pm 0.2) \times 10^{18}$
n-$C_{20}H_{42}$	$(1.6 \pm 0.2) \times 10^{18}$
n-$C_{36}H_{74}$	$(1.1 \pm 0.1) \times 10^{16}$

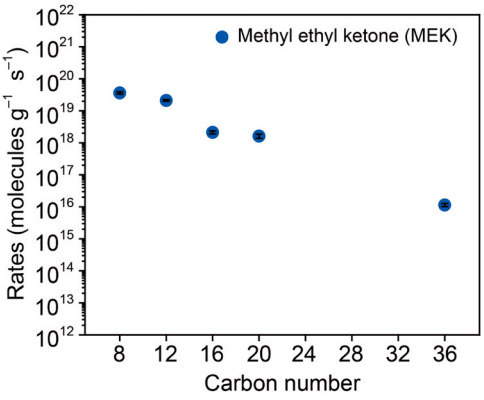

Fig. 3. Oxidation activity for linear alkanes ranging from octane (n-C_8H_{18}) to hexatriacontane (n-$C_{36}H_{74}$) in methyl ethyl ketone. (Error bars indicate standard deviation.).

Table 3
Oxidation rates of dodecane in methanol, acetone, ACN, MEK and MBK, plotted as a function of partition coefficients.

Cosolvent	Dodecane oxidation rate (molecules g^{-1} s^{-1})	Octanol–water partition coefficient (P)[a]
Methanol	0	0.32
Acetone	0	0.36
Acetonitrile	2.4×10^{17}	0.58
Methyl ethyl ketone	2.1×10^{19}	2.0
Methyl butyl ketone	2.8×10^{19}	20

[a] P was estimated from the calculated octanol-water partition coefficients in reference [26].

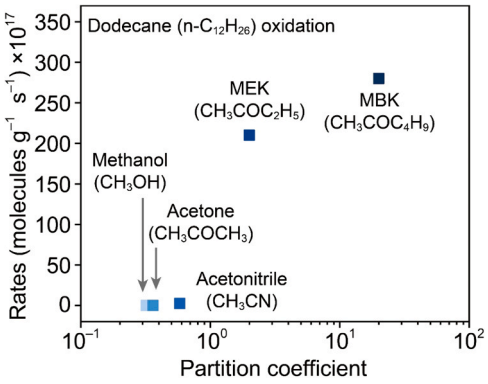

Fig. 4. Oxidation rates of dodecane (n-$C_{12}H_{26}$) in methanol, acetonitrile, MEK and MBK, plotted as a function of partition coefficients.

between the coefficients and the rates indicate that cosolvents with higher partition coefficients would facilitate alkane transport to the water-rich phase[27,28] that contained the catalyst.

The dependence of rates on alkane size could also be due to diffusion limitations, since diffusion coefficients for larger hydrocarbons will be much smaller. Because diffusion limitations should be greater for larger TS-1 crystallites, we compared rates for several of the alkanes on TS-1 (420), a sample with 420-nm crystallites, to those on TS-1(190), the sample with 190-nm crystallites. As shown in Fig. 5, rates were approximately 3 times lower on the TS-1(420) sample. However, this difference in rates was the same for all three alkanes. This result is consistent with TS-1(420) having a site concentration that is three times lower than that of TS-1(190), independent of whether or not diffusion limits reaction. The fact that both n-$C_{12}H_{26}$ and n-$C_{36}H_{74}$ show the same difference in rates implies that reaction is either diffusion-limited for both reactants in both catalysts or for neither reactant in either catalyst.

To investigate if external mass transfer may be affecting the reaction rate, we measured the hexadecane oxidation rate over the 190 nm TS-1 using stirring rates of 50 rpm and 200 rpm. The rates were found to be similar indicating that external mass transfer was not limiting for the reaction conditions used in this study.

To determine whether diffusion is likely to be limiting, we performed an estimate of the Thiele Modulus for n-$C_{12}H_{26}$ on TS-1(190), with MEK as cosolvent. Using the reported diffusivity for n-$C_{12}H_{26}$ of 7×10^{-12} m^2/s[29], the characteristic time for diffusion in the 190-nm zeolite crystallites (radius, R, is 95 nm), R^2/D, is ~0.0013 s. To determine if the reaction is diffusion-limited, the characteristic diffusion time should be compared to the characteristic reaction time, k^{-1}. This reaction time can be approximated by C_o/r[30], where C_o is the concentration of the alkane in the aqueous phase, and r is the consumption rate of the alkane per volume of catalyst. The consumption rate in the catalyst can be

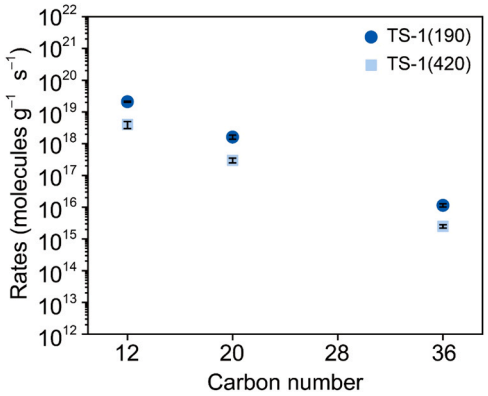

Fig. 5. Oxidation rates of n-$C_{12}H_{26}$, n-$C_{20}H_{42}$, and n-$C_{36}H_{74}$ in MEK at 348 K.

determined by multiplying the rate in Table 2 by the density of the catalyst, ~1.5 g/cm^3. The concentration of n-$C_{12}H_{26}$ in a water-MEK mixture at 348 K is unknown but certainly greater than the equilibrium concentration of n-$C_{12}H_{26}$ in pure water at room temperature, 2.1×10^{-5} mol/l[31]. Using these values gives a Thiele Modulus $(kR^2/D)^{½}$ of 1.8. A similar analysis for TS-1(420) gives a Thiele Modulus of 2.3. While these values are slightly greater than 1, which is often used as the point where diffusion limitations start to be significant, these values should be considered upper limits since the C12 concentration in the water/MEK phase will be higher than that of C12 in pure water. Taking this into account, the Thiele modulus analysis indicates that diffusional limitations should not be significant. If diffusion is not limiting for n-$C_{12}H_{26}$, the results in Fig. 5 imply that diffusion is also not limiting for n-$C_{36}H_{74}$.

Finally, the effect of reaction temperature was studied for the oxidation of n-$C_{20}H_{42}$ between 328 K and 358 K, with an Arrhenius plot shown in Fig. 6. As expected, rates increased with temperature. The activation energy for the reaction was 85 ± 13 kJ/mol.

3.2. Product identification

While the GC-MS measurements showed that alkane oxidation had occurred and that difunctional products were formed only at higher conversions, they did not provide detailed information on the nature of the products. Therefore, ^{1}H NMR measurements were performed on the products. We investigated products obtained using acetonitrile as the cosolvent since the carbonyl groups in MEK and MBK interfered with signal from oxidation products; because the conversions with n-$C_{36}H_{74}$ were low, only measurements with n-C_8H_{18} to n-$C_{20}H_{42}$ are reported. The spectrum for oxidation of n-$C_{16}H_{34}$ is shown in Fig. 7, while spectra for the oxidation products from the other alkanes are reported in Figures S6 through S8 of the Supporting Information. Notably, reference hydrocarbon samples showed proton peaks related to methylene and methyl groups without indication of ketone and alcohol formation. The selectivity for alcohols and ketones was calculated from the characteristic ^{1}H NMR signals at approximately 2.1–2.4 ppm for alpha keto protons in methyl ketones and ketones (–CH_2–CO–CH_3 and –CH_2–CO–CH_2–), and 3.5 ppm for alpha protons in alcohols (–CH–OH). As shown in Fig. 8a, more than 80 % of the products formed from each of the alkanes were ketones. Because there was no signal at 9–10 ppm, the ^{1}H NMR spectra indicate that no aldehydes were formed.

To confirm the presence of alcohol and ketone products, we obtained 2D NMR spectra using Heteronuclear Multiple Bond Correlation (HMBC) and Heteronuclear Single Quantum Coherence (HSQC) experiments. The spectra in Figures S9 through S12 show features associated with both ketones and alcohols following reaction of n-C_8H_{18} and n-$C_{12}H_{26}$. HMBC experiments further confirmed ketone formation from n-$C_{16}H_{34}$ oxidation, as shown in Fig. S13. Although the alcohol peaks in the HSQC experiments were initially too small to display in Fig. S14a, an enlarged image in Fig. S14b clearly revealed their presence. These results demonstrate that both ketones and alcohols are oxidation products of alkane, with ketones formed in significantly higher amounts. Due to the very small peaks observed for n-$C_{16}H_{34}$ in the HSQC spectra, we did not extend the experiments to n-$C_{20}H_{42}$, although we expect similar production of alcohols and ketones, as observable in ^{1}H NMR spectra.

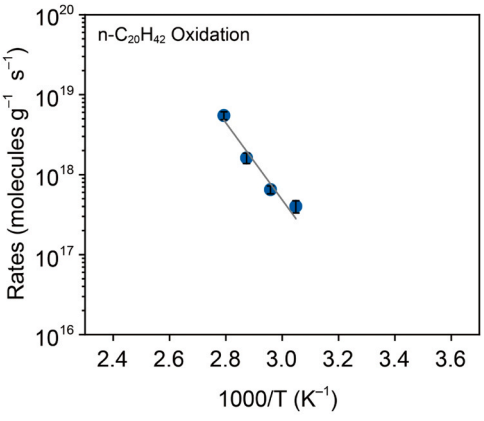

Fig. 6. Arrhenius plot for n-$C_{20}H_{42}$ oxidation in MEK conducted at 328, 338, 348 and 358 K.

It is also important to determine whether oxidation occurs randomly at the internal carbons of the alkane chain. Specifically, the alpha keto protons in the methyl group of methyl ketone (R–CO–CH_3) give a signal at 2.1 ppm while those in the methylene group of methyl ketone and ketone (R–CH_2–CO–CH_2–R) resonate at 2.4 ppm. By analyzing the areas of these peaks and the number of protons, we estimated the proportion of methyl ketones relative to internal ketones. The values obtained for n-C_8H_{18} to $C_{20}H_{40}$ are shown in Fig. 8b, together with the statistical result expected if all internal carbons react with equal probability. Fig. 8b shows that there clearly is preferential reaction at the 2 positions, as others have also reported[32,33]; but oxidation is not restricted to those carbons.

Because internal carbons are less reactive than carbons at the 2 position, the lower reactivity of large alkanes could be due in part to the lower fraction of 2 carbons in the larger alkanes. To account for this, it is reasonable to assume that the reactivity of internal carbons relative to those in the 2 position is proportional to the selectivity (Table 4 and Fig. 9). While the carbons at the 2 position clearly appear to be more reactive, the difference in reactivities is not large enough to explain the large differences in rates for alkanes of different sizes. For n-$C_{12}H_{26}$, the rate of C_2 is an order of magnitude higher than that of internal carbons although this difference is smaller for n-C_8H_{18}. The difference in relative rates between C_2 and internal carbons diminishes for n-$C_{16}H_{34}$, and n-$C_{20}H_{42}$. This trend is important for application to polymers, since functionalization of internal carbons is desired.

4. Discussion

We have demonstrated that the direct functionalization of large alkanes using H_2O_2 and a titanium-silicate catalyst produces functionalized products and showed the critical role of cosolvent in enhancing the reaction rates. The oxidation reactions are highly selective for producing alcohols and ketones and there was no evidence for carbon-carbon bond breaking. Reaction occurred more selectively at the 2-positions in the alkane, but oxidation at other positions in the chain was also observed. Expanding these results to polyolefin upcycling, it would be desirable to enhance the reaction rate at the central carbons. The relatively inexpensive catalyst and reactants also make this process potentially attractive.

Obviously, higher rates would be desirable. The limiting factor appears to be that H_2O_2 and alkane are distributed between separate water-rich and organic-rich phases, with the solid catalyst predominantly residing in the water-rich phase. Cosolvents that enhance the partitioning of alkane in the aqueous phase significantly increase the reaction rates. Thus, the identification of better cosolvents represents a target of opportunity. Alternatively, there may be other methods for achieving conditions in which the two reactants and the catalyst are present in the same phase.

While our results suggest that the reaction rates were not limited by diffusion within the TS-1 zeolite crystallites for the molecules studied here, transport limitations will become more important for larger alkanes. Note, however, that studies using ZSM-5 zeolite for dewaxing petroleum fractions [34,35] provide evidence that even relatively large alkanes can diffuse into zeolite pores. A recent study of oxidative conversion of polyethylene over TS-1 also suggests that polymeric substrates can react within the TS-1 framework [36]. Nonetheless it is likely that reaction of polyethylene chains in TS-1 pores will be highly diffusion limited. Since rates for diffusion-limited reactions can be increased

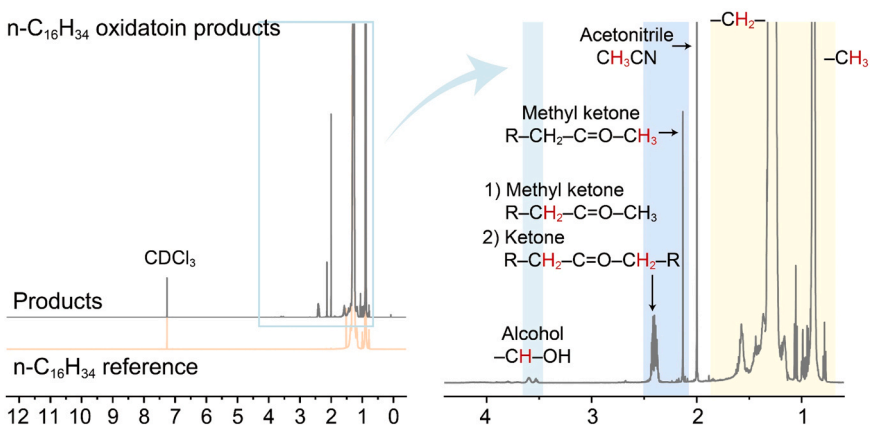

Fig. 7. ^{1}H NMR spectra of hexadecane (n-$C_{16}H_{34}$) oxidation products.

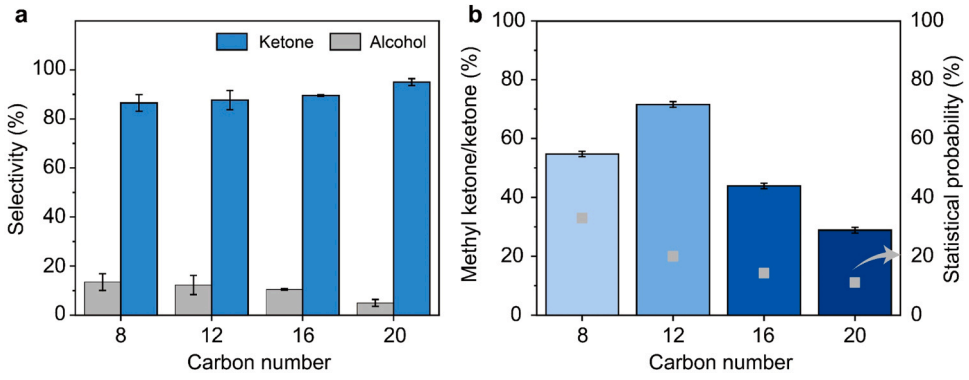

Fig. 8. (a) Selectivity of ketones and alcohols, and (b) ratios of methyl ketone among ketone derivatives across alkanes ranging from n-C_8H_{18} to n-$C_{36}H_{74}$ reacted with acetonitrile cosolvent. (Error bars indicate standard deviation.).

Table 4
Estimated reaction rates for ketones with carbonyl groups located on C_2 and other carbons.

Reactant	Rate (molecules g^{-1} s^{-1})		Carbon-Normalized Rate (molecules g^{-1} s^{-1} $carbon^{-1}$)	
	Second carbon	Internal carbons	Second carbon	Internal carbons
n-C_8H_{18}	2.7×10^{17}	2.2×10^{17}	1.3×10^{17}	5.5×10^{16}
n-$C_{12}H_{26}$	1.5×10^{17}	6.0×10^{16}	7.6×10^{16}	7.5×10^{15}
n-$C_{16}H_{34}$	2.7×10^{16}	3.5×10^{16}	1.4×10^{16}	2.9×10^{15}
n-$C_{20}H_{42}$	9.5×10^{15}	2.3×10^{16}	4.7×10^{15}	1.5×10^{14}

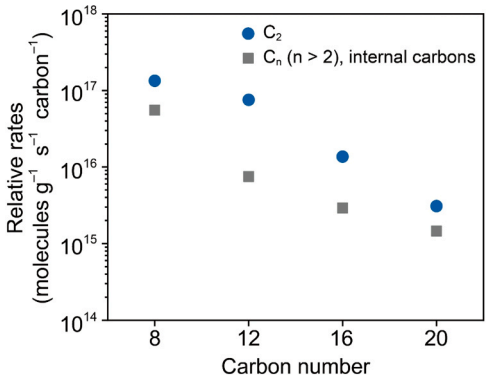

Fig. 9. Reaction rates for ketone products with different locations of carbonyl groups in the alkane chains.

by decreasing the length scale of the catalyst, to apply the chemistry explored in this study to polyethylene it may be necessary to use catalysts with larger pores than TS-1 or use "hierarchical" TS-1 catalysts [37, 38] which have most of the active sites at the external surfaces. This strategy has been employed in hydrogenolysis of polyolefins over zeolites to overcome diffusion limitations [39,40]. Alternatively, reactor designs that optimize intimate contact between immiscible phases have been reported [41–44].

While the present study examined some relatively large alkanes, polyolefins will represent additional challenges. Their high melting temperatures and melt viscosities will further complicate the contacting issues observed here. However, the increased product value that could be achieved makes the effort worthwhile.

5. Conclusions

The mild oxidation of linear alkanes into ketones and alcohols can be achieved using TS-1 catalysts and H_2O_2. Our reactivity tests across alkanes ranging from n-C_8H_{18} to n-$C_{36}H_{74}$ in different cosolvents suggest

that alkane concentrations in the aqueous phase significantly impact the oxidation rates in the biphasic reactant medium. Additionally, the 2 position of alkane chains is a preferential reaction site while the oxidation also proceeds at central carbon positions.

CRediT authorship contribution statement

Seyeon Park: Writing – review & editing, Writing – original draft, Methodology, Investigation, Formal analysis. **Zhuoming Feng:** Investigation, Formal analysis. **Maura Gibbs:** Investigation, Formal analysis. **Goldberg Karen:** Supervision. **Gorte Raymond:** Writing – review & editing, Supervision, Project administration. **Daeyeon Lee:** Supervision. **Vohs John Michael:** Writing – review & editing, Supervision, Project administration, Funding acquisition.

Declaration of Competing Interest

The authors declare that they have no known competing financial interests or personal relationships that could have appeared to influence the work reported in this paper.

Acknowledgements

This work was supported by the Department of Energy, Office of Basic Energy Sciences (Grant No. DE-SC0022238).

Appendix A. Supporting information

Supplementary data associated with this article can be found in the online version at doi:10.1016/j.apcata.2025.120378.

Data availability

Data will be made available on request.

References

[1] P.A. Kots, T.J. Xie, B.C. Vance, C.M. Quinn, M.D. de Mello, J.A. Boscoboinik, C. Wang, P. Kumar, E.A. Stach, N.S. Marinkovic, L. Ma, S.N. Ehrlich, D.G. Vlachos, Electronic modulation of metal-support interactions improves polypropylene hydrogenolysis over ruthenium catalysts, Nat. Commun. 13 (2022).
[2] S. Lee, K. Shen, C.Y. Wang, J.M. Vohs, R.J. Gorte, Hydrogenolysis of n-eicosane over Ru-based catalysts in a continuous flow reactor, Chem. Eng. J. 456 (2023).
[3] S.B. Liu, P.A. Kots, B.C. Vance, A. Danielson, D.G. Vlachos, Plastic waste to fuels by hydrocracking at mild conditions, Sci. Adv. 7 (2021).
[4] J.Z. Tan, C.W. Hullfish, Y.T. Zheng, B.E. Koel, M.L. Sarazen, Conversion of polyethylene waste to short chain hydrocarbons under mild temperature and hydrogen pressure with metal-free and metal-loaded MFI zeolites, Appl. Catal. B-Environ. 338 (2023).
[5] F. Zhang, M.H. Zeng, R.D. Yappert, J.K. Sun, Y.H. Lee, A.M. LaPointe, B. Peters, M. M. Abu-Omar, S.L. Scott, Polyethylene upcycling to long-chain alkylaromatics by tandem hydrogenolysis/aromatization, Science 370 (2020) 437–441.
[6] J.E. Rorrer, G.T. Beckham, Y. Román-Leshkov, Conversion of polyolefin waste to liquid alkanes with Ru-based catalysts under mild conditions, Jacs Au 1 (2021) 8–12.
[7] L.Y. Chen, K.G. Malollari, A. Uliana, D. Sanchez, P.B. Messersmith, J.F. Hartwig, Selective, catalytic oxidations of C-H bonds in polyethylenes produce functional materials with enhanced adhesion, Chem. Us 7 (2021) 137–145.
[8] J.K. Sun, J.H. Dong, L.J. Gao, Y.Q. Zhao, H. Moon, S.L. Scott, Catalytic upcycling of polyolefins, Chem. Rev. 124 (2024) 9457–9579.
[9] J.X. Shi, N.R. Ciccia, S. Pal, D.D. Kim, J.N. Brunn, C. Lizandara-Pueyo, M. Ernst, A. M. Haydl, P.B. Messersmith, B.A. Helms, J.F. Hartwig, Chemical modification of oxidized polyethylene enables access to functional polyethylenes with greater reuse, J. Am. Chem. Soc. 145 (2023) 21527–21537.
[10] A. Bunescu, S.W. Lee, Q. Li, J.F. Hartwig, Catalytic hydroxylation of polyethylenes, ACS Cent. Sci. 3 (2017) 895–903.
[11] M. Miceli, P. Frontera, A. Macario, A. Malara, Recovery/reuse of heterogeneous supported spent catalysts, Catalysts 11 (2021).
[12] S.T. Bai, G. De Smet, Y. Liao, R. Sun, C. Zhou, M. Beller, B.U.W. Maes, B.F. Sels, Homogeneous and heterogeneous catalysts for hydrogenation of CO_2 to methanol under mild conditions, Chem. Soc. Rev. 50 (2021) 4259–4298.
[13] D.R.C. Huybrechts, L. Debruycker, P.A. Jacobs, Oxyfunctionalization of alkanes with hydrogen-peroxide on titanium silicalite, Nature 345 (1990) 240–242.
[14] C.B. Khouw, C.B. Dartt, J.A. Labinger, M.E. Davis, Studies on the catalytic-oxidation of alkanes and alkenes by titanium silicates, J. Catal. 149 (1994) 195–205.
[15] G.M. Kuz'micheva, R.D. Svetogorov, E.V. Khramov, G.V. Kravchenko, L.G. Bruk, Z. Y. Pastukhova, E.B. Markova, A.I. Zhukova, S.G. Chuklina, A.V. Dorokhov, Titanosilicalites (MFI-type): composition, statistical and local structure, catalytic properties, Micro Mesopor Mat. 326 (2021).
[16] R. Millini, G. Bellussi, P. Pollesel, C. Rizzo, C. Perego, Beyond TS-1: background and recent advances in the synthesis of Ti-containing zeolites, Micro Mesopor Mat. 346 (2022).
[17] M.G. Clerici, The role of the solvent in TS-1 chemistry: active or passive? An early study revisited, Top. Catal. 15 (2001) 257–263.
[18] J.E. Gallot, H. Fu, M.P. Kapoor, S. Kaliaguine, Kinetic modeling of n-hexane oxyfunctionalization by hydrogen peroxide on titanium silicalites of MEL structure (TS-2), J. Catal. 161 (1996) 798–809.
[19] S. Danov, A. Fedosov, A. Lunin, Liquid-phase oxidation of normal C 10–C 13 hydrocarbons with hydrogen peroxide on the titanium-containing catalyst ts-1: the effect of process conditions on product composition, Catal. Ind. 2 (2010) 239–245.
[20] Y.H. Yeh, R.J. Gorte, S. Rangarajan, M. Mavrikakis, Adsorption of small alkanes on ZSM-5 zeolites: influence of bronsted sites, J. Phys. Chem. C. 120 (2016) 12132–12138.
[21] C.Y. Chen, S.I. Zones, Investigation of small-pore zeolites via vapor-phase adsorption of n-hexane, Chem. Ing. Tech. 93 (2021) 959–966.
[22] F. Bonino, A. Damin, G. Ricchiardi, M. Ricci, G. Spanò, R. D'Aloisio, A. Zecchina, C. Lamberti, C. Prestipino, S. Bordiga, Ti-peroxo species in the TS-1/H_2O_2/H_2O system, J. Phys. Chem. B 108 (2004) 3573–3583.
[23] D.T. Bregante, A.M. Johnson, A.Y. Patel, E.Z. Ayla, M.J. Cordon, B.C. Bukowski, J. Greeley, R. Gounder, D.W. Flaherty, Cooperative effects between hydrophilic pores and solvents: catalytic consequences of hydrogen bonding on alkene epoxidation in zeolites, J. Am. Chem. Soc. 141 (2019) 7302–7319.
[24] Q.H. Zhu, M.N. Liang, W.J. Yan, W.H. Ma, Effective hierarchization of TS-1 and its catalytic performance in propene epoxidation, Micro Mesopor Mat. 278 (2019) 307–313.
[25] W.B. Fan, P. Wu, T. Tatsumi, Unique solvent effect of microporous crystalline titanosilicates in the oxidation of 1-hexene and cyclohexene, J. Catal. 256 (2008) 62–73.
[26] D.E. Leahy, Intrinsic molecular volume as a measure of the cavity term in linear solvation energy relationships: octanol-water partition coefficients and aqueous solubilities, J. Pharm. Sci. Us 75 (1986) 629–636.
[27] A.W. Islam, A. Javvadi, V.N. Kabadi, Universal liquid mixture models for vapor−liquid and liquid−liquid equilibria in the hexane−butanol−water system, Ind. Eng. Chem. Res. 50 (2011) 1034–1045.
[28] R.M. Suzuki, M.C. Sérgi Gomes, J.G. Sgorlon, R. Oliveira Defendi, A.C. Raimundini Aranha, C.C. Sipoli, Reusing a residue from the juice industry: extraction of oil from passion fruit seeds and its incorporation into liposomes, J. Chem. Technol. Biotechnol. 99 (2024) 685–694.
[29] H. Jobic, W. Schmidt, C.B. Krause, J. Kärger, PFG NMR and QENS diffusion study of n-alkane homologues in MFI-type zeolites, Micro Mesopor Mat. 90 (2006) 299–306.
[30] H. Fu, S. Kaliaguine, A kinetic investigation of co-solvent effects in oxyfunctionalization of n-hexane by hydrogen-peroxide on TS-2, J. Catal. 148 (1994) 540–549.
[31] D.G. Shaw, Hydrocarbons with water and seawater, Pergamon Press Oxford, 1989.
[32] R.H.P.R. Poladi, C.C. Landry, Oxidation of octane and cyclohexane using a new porous substrate, Ti-MMM-1, Micro Mesopor Mat. 52 (2002) 11–18.
[33] G.B. Shul'pin, T. Sooknoi, V.B. Romakh, G. Süss-Fink, L.S. Shul'pina, Regioselective alkane oxygenation with H_2O_2 catalyzed by titanosilicalite TS-1, Tetrahedron Lett. 47 (2006) 3071–3075.
[34] D.J. O'Rear, B.K. Lok, Kinetics of dewaxing neutral oils over Zsm-5, Ind. Eng. Chem. Res 30 (1991) 1100–1105.
[35] S. Sivasanker, K.J. Waghmare, K.M. Reddy, A.N. Kothasthane, P. Ratnasamy, The influence of physicochemical properties of Zsm-5 on catalytic dewaxing, J. Chem. Technol. Biot. 48 (1990) 261–268.
[36] X.Y. Hou, F. Yuan, X.D. Liu, K.L. Wang, Y. Zhu, P. Cheng, R.R. Jia, L.Y. Shi, L. Huang, Gradient-temperature control enhances oxi-upcycling of polyethylene plastics to dicarboxylic acids over TS-1 zeolite, Chem. Eng. J. 504 (2025).
[37] R.S. Bai, Y. Song, L. Lätsch, Y.C. Zou, Z.C. Feng, C. Copéret, A. Corma, J.H. Yu, Switching between classical/nonclassical crystallization pathways of TS-1 zeolite: implication on titanium distribution and catalysis, Chem. Sci. 13 (2022) 10868–10877.
[38] M. Zhang, S.Y. Ren, Q.X. Guo, B.J. Shen, Synthesis of hierarchically porous zeolite TS-1 with small crystal size and its performance of 1-hexene epoxidation reaction, Micro Mesopor Mat. 326 (2021).
[39] J.Z. Tan, M. Ortega, S.A. Miller, C.W. Hullfish, H. Kim, S. Kim, W.D. Hu, J.Z. Hu, J. A. Lercher, B.E. Koel, M.L. Sarazen, Catalytic consequences of hierarchical pore architectures within MFI and FAU Zeolites for polyethylene conversion, ACS Catal. 14 (2024) 7536–7552.
[40] S. Wang, W.C. Wang, M.Y. Chu, D.W. Gao, Y. Wang, Y.P. Lv, R.Y. Wang, L.H. Song, H.Q. Zhao, J.X. Chen, G.Z. Chen, Ultra-narrow alkane product distribution in polyethylene waste hydrocracking by zeolite micro-mesopore diffusion optimization, Angew. Chem. Int Ed. 63 (2024).
[41] P. Desir, D.G. Vlachos, Intensified reactive extraction for the acid-catalyzed conversion of fructose to 5-hydroxymethyl furfural, Chem. Eng. J. 428 (2022).

[42] P. Desir, B. Saha, D.G. Vlachos, Ultrafast flow chemistry for the acid-catalyzed conversion of fructose, Energ. Environ. Sci. 12 (2019).
[43] S. Ahn, S.L. Nauert, K.E. Hicks, M.A. Ardagh, N.M. Schweitzer, O.K. Farha, J. M. Notestein, Demonstrating the critical role of solvation in supported Ti and Nb epoxidation catalysts via vapor-phase kinetics, ACS Catal. 10 (2020) 2817–2825.
[44] Y. Kon, T. Nakashima, Y. Makino, H. Nagashima, S.Y. Onozawa, S. Kobayashi, K. Sato, Continuous synthesis of epoxides from alkenes by hydrogen peroxide with titanium silicalite-1 catalyst using flow reactors, Adv. Synth. Catal. 365 (2023) 3227–3233.